

# Curcumin@Fe/Tannic Acid Complex Nanoparticles for Inflammatory Bowel Disease Treatment

Jiman Jin, Xiuzhi Ye, Zhenfeng Huang, Shicui Jiang,\* and Dini Lin\*

Cite This: *ACS Omega* 2024, 9, 14316–14322

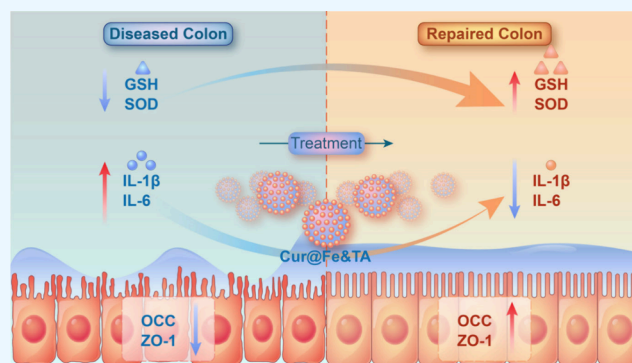
Read Online

ACCESS |

Metrics &amp; More

Article Recommendations

**ABSTRACT:** Inflammatory bowel disease (IBD) is a serious public health issue because of its chronic and incurable nature. Common IBD drugs have limited efficacy and produce adverse effects, leading to an urgent need to develop new drugs and drug delivery systems. Curcumin (Cur) is a natural and nontoxic drug that is increasingly used in the treatment of IBD owing to its anti-inflammatory and antioxidant effects. Metal–polyphenol networks constructed from metal ions and polyphenols exhibit biological functionality while acting as an adhesive nanomaterial to encapsulate nano-Cur, thereby improving its solubility and drug release behavior. In this study, we prepared a Cur@Fe&TA nanodrug delivery system by constructing an Fe<sup>3+</sup>/tannic acid (TA) metal–polyphenol network with encapsulated Cur. The Cur@Fe&TA nanodrug exhibited good stability, drug release behavior, and biocompatibility. Based on the anti-inflammatory and antioxidant effects of Cur@Fe&TA, the gastrointestinal cytopathology in an IBD mouse model was effectively improved. The proposed Cur@Fe&TA nanomedicine delivery system has promising application and research value for the treatment of IBD by regulating levels of antioxidants and inflammatory cytokines.



## 1. INTRODUCTION

Inflammatory bowel disease (IBD) is a chronic inflammatory condition of the gastrointestinal tract. Common complications include persistent inflammation, intestinal lesions, particularly of the colorectal and rectal mucosa and submucosa,<sup>1–4</sup> and gastrointestinal fibrosis, which can seriously affect patients' quality of life.<sup>5,6</sup> The etiology and pathogenesis of IBD are not fully understood; however, current research suggests that it is a multigenic disease associated with abnormal immune function, intestinal infections, genetic factors, intestinal flora, and other factors.<sup>7–9</sup> Clinical treatments for IBD include anti-inflammatory drugs and biopharmaceuticals to reduce colonic mucosal and systemic inflammation and regulate the immune response. However, owing to the chronic nature of IBD and the adverse side effects of these drugs, the clinical effectiveness of IBD treatments is limited.<sup>5,10</sup> Consequently, there is an urgent need for further research and development of appropriate drugs and drug delivery systems.

Curcumin (Cur) is a natural nontoxic drug that is increasingly used to treat IBD owing to its anti-inflammatory and antioxidant effects.<sup>11–13</sup> Cur inhibits major inflammatory mechanisms, such as cyclooxygenase 2, lipoxygenase, tumor necrosis factor  $\alpha$ , interferon  $\gamma$ , and nuclear factor  $\kappa$ B expression,<sup>13–15</sup> and has been shown to regulate intestinal flora.<sup>16</sup> However, the efficacy and clinical use of Cur are hindered by its insolubility in water, low accumulation at inflammation sites after oral administration, and

short retention time.<sup>17–19</sup> To overcome these limitations, we constructed a nanodrug delivery system by wrapping Cur with a metal–polyphenol network. Metal–polyphenol networks constructed from metal ions and polyphenols exhibit biological functionality. For example, the Fe<sup>3+</sup>/tannic acid (TA) network has been shown to exert good antimicrobial and antioxidant effects.<sup>20</sup> Metal–polyphenol networks also exhibit adhesion-based encapsulation behavior owing to physicochemical interactions (e.g., cation– $\pi$  and coordination interactions) between the metal cation and polyphenol.<sup>21</sup> Encapsulating Cur in a Fe<sup>3+</sup>/TA metal–polyphenol network is expected to improve the solubility and drug release behavior of Cur and expand its clinical application.<sup>22–27</sup> All the components of the Cur@Fe&TA nanodrug delivery system are pharmacologically active, thereby reducing the use of nontherapeutic excipients.<sup>25,28</sup> Moreover, this multidrug nanodrug delivery system is expected to promote the treatment of IBD through synergistic therapeutic effects.<sup>29,30</sup>

Received: December 20, 2023

Revised: January 25, 2024

Accepted: March 5, 2024

Published: March 14, 2024



We prepared the Cur@Fe&TA nanodrug delivery system by a simple encapsulation strategy. First, nanostructured Cur was prepared via sonication, and then Fe<sup>3+</sup> and TA were successively introduced under sonication to construct a metal–polyphenol network. This network wrapped around the nano-Cur particles to form a Cur@Fe&TA core@shell structure. *In vitro* and *in vivo* experiments demonstrated that the Cur@Fe&TA drug delivery system had good biocompatibility and sustained and stable drug release behavior. Moreover, the drug delivery system could regulate the expression of various oxidative and inflammatory factors, such as SOD, GSH, and IL-6 in gastrointestinal cells of an IBD mouse model, thus promoting IBD treatment (Figure 1).

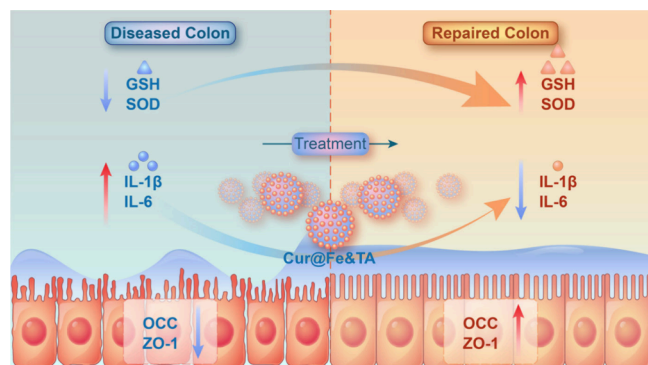


**Figure 1.** Mechanism of Cur@Fe&TA nanoparticles for the treatment of IBD.

The results also demonstrated the synergistic therapeutic effect of the multidrug nanodrug delivery system. The proposed Cur@Fe&TA drug delivery system effectively improves the inflammatory and oxidative activities of the intestinal tract, thus promoting the treatment of IBD. The proposed Cur@Fe&TA drug delivery system has excellent clinical and research significance.

## 2. RESULTS

**2.1. Characterization of Cur@Fe&TA.** The successful encapsulation of Cur in the metal–polyphenol Fe/TA network was analyzed based on the stability of its aqueous solution. CHCl<sub>3</sub> is a good organic solvent that can quickly dissolve Cur, so aqueous solutions of Cur diffuse into CHCl<sub>3</sub>. By contrast, if the prepared nanomaterials are stable in water, their aqueous solutions will not diffuse into CHCl<sub>3</sub>. As shown in Figure 2a, when a Cur aqueous solution was dropped into CHCl<sub>3</sub>, the solutions diffused into each other, whereas the layers remained separated when using a Cur@Fe&TA aqueous solution. This confirms that the prepared nanomaterials had good stability in water.<sup>31</sup>

The morphology of the Cur@Fe&TA powder was observed by scanning electron microscopy (SEM). The particle diameter was approximately 150–250 nm (Figure 2b). Observation of the fine structure of Cur@Fe&TA by transmission electron microscopy (TEM) shows that the nanomaterial is similar to a circular shape. Elemental analysis also showed that the Cur@Fe&TA contained Fe and O (Figure 2c). The particle size and zeta potential of the Cur@Fe&TA solution were directly measured using dynamic light scattering (DLS). The particle size distribution was similar to that observed by SEM, with a peak particle size of 191.7 nm (Figure 2d). Because organisms' cell membranes comprise anionic phospholipid bilayers, positively charged nanomaterials are more likely to trigger an

immune response and cytotoxicity, whereas negatively charged nanomaterials have higher biological safety.<sup>32</sup> The zeta potential of Cur@Fe&TA was −24.9 mV. This negative zeta potential indicates that it should have low cytotoxicity. In addition, since the absolute zeta potential is greater than ±15 mV, individual nanoparticles will experience a certain repulsion, which should hinder particle aggregation (Figure 2e). In addition, the drug loading rate and encapsulation rate of the prepared Cur@Fe&TA are also closely related to its practical application. After measuring the nanomaterial and calculating the data, it was concluded that the drug loading rate of Cur@Fe&TA was close to 40%, while the encapsulation rate was close to 35%.

**2.2. Biocompatibility of Cur@Fe&TA.** The cytotoxicity of metallic nanomaterials is the main obstacle to their clinical use. To evaluate the biocompatibility of the Cur@Fe&TA metal–polyphenol drug delivery system, bone-marrow-derived stem cells (BMSCs) were used as a model cell line. BMSCs were cocultured with Cur@Fe&TA, Cur, Fe&TA, or phosphate-buffered saline (PBS) for 24 h and then stained with Calcein AM/PI to detect cell death. In addition, cell viability after cocultivation with each drug for three consecutive days was detected by cell counting kit (CCK)-8 assay. The results showed that Cur@Fe&TA does not cause significant cell death, with all BMSC groups surviving after cocultivation with the drugs (Figure 3a). Additionally, the Cur@Fe&TA composite nanomedicine did not significantly alter cellular activity; that is, there were no statistically significant differences in the CCK-8 assay results between the experimental and control (PBS) groups (Figure 3b).

**2.3. Drug Release from Cur@Fe&TA.** Patients with IBD usually have complex gastrointestinal lesions, and conventional oral IBD therapeutic drugs can have limited long-term therapeutic effects owing to their rapid degradation and release. Thus, IBD therapeutic drugs should ideally exhibit a stable and sustained drug release. We measured the *in vitro* release of Cur from Cur@Fe&TA nanoparticles using ultraviolet (UV) spectrophotometry and found that Cur@Fe&TA was capable of sustained drug release in PBS at 37 °C (Figure 4). The amount of Cur released increased gradually for approximately 20 h before stabilizing.

**2.4. *In Vivo* Therapeutic Effect of Cur@Fe&TA.** The therapeutic effect of Cur@Fe&TA was analyzed *in vivo* using an IBD mouse model in which colitis was induced by administering dextran sodium sulfate (DSS). The body weight and colon length of mice under different treatment conditions were directly assessed as an indicator of the effectiveness of treatment. In general, the smaller the change in body weight, the more effective the treatment. Furthermore, if drug treatment is effective, the colon length should be similar to that of the control group (Figure 5a). The experimental results showed that mice without DSS induction (control group) showed an increase in body weight, while those with DSS induction all showed a significant decrease in body weight, with the exception of the Cur@Fe&TA group, which showed only a slight decrease in body weight (Figure 5b). Furthermore, colon length comparisons revealed that the Cur@Fe&TA group had the closest colon lengths to those of the control group (Figure 5c).

Tissue hematoxylin and eosin (H&E) staining is an important indicator for evaluating the *in vivo* safety of nanodrugs as well as the therapeutic efficacy of different dosing groups. At the end of the treatment cycle, the mice were dissected, and the target colon tissues were removed for H&E staining, the results of which were scored for pathology. The pathological condition of

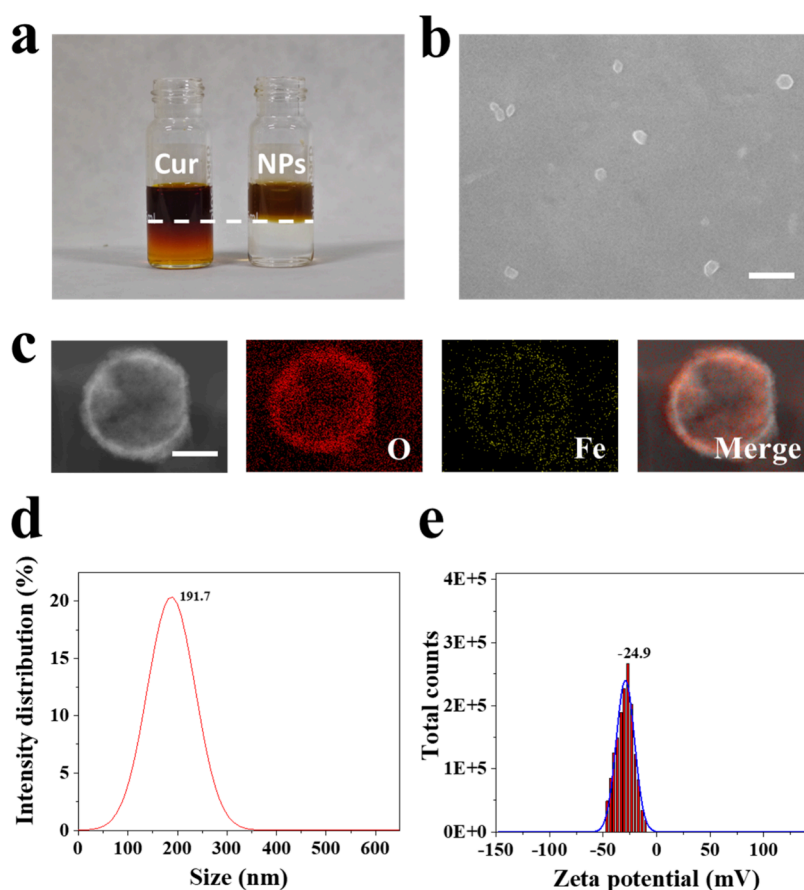


**Figure 2.** Characterization of Cur@Fe&TA. (a) Stability of Cur and Cur@Fe&TA aqueous solutions. Aqueous Cur solution promptly diffused into the  $\text{CHCl}_3$  layer (left) while aqueous Cur@Fe&TA solution exhibited distinct separation (right). (b) SEM image of Cur@Fe&TA powder. Scale bar: 500 nm. (c) TEM image of Cur@Fe&TA powder. Scale bar: 100 nm. (d) Particle size distribution and (e) zeta potential of Cur@Fe&TA as determined by DLS.

the mice colons treated with each drug was better than that of mice with no treatment (DSS group), confirming that the Cur@Fe&TA drug delivery system had a good therapeutic effect (Figure 6a).

**2.5. *In Vivo* Antiapoptotic and Anti-inflammatory Effect of Cur@Fe&TA.** Immunofluorescence staining was used to detect the secretion of various cytokines by intestinal mucosal epithelial cells in the IBD mouse model. Terminal deoxynucleotidyl transferase-mediated dUTP nick end-labeling (TUNEL) immunofluorescence showed that the DSS group exhibited significant apoptosis, owing to the destructive effect of IBD on the intestinal mucosa. However, drug treatment reduced apoptosis in the intestinal mucosa (Figure 6b). Zonula occludens (ZO)-1 and 3,3-dipentylloxycarbocyanine (OCC) fluorescence staining also confirmed that the condition of the colonic barrier in the Cur@Fe&TA group was similar to that of the control group (Figure 7a). Quantitative analysis of the fluorescence intensity was performed, and the results again verified the therapeutic effect of Cur@Fe&TA (Figure 7b,c). These results confirm that the Cur@Fe&TA nanodrug delivery system reduces apoptosis and improves the mucosal barrier condition in IBD mouse intestinal mucosal cells, thereby promoting healing.

**2.6. Cur@Fe&TA Regulation of Inflammation and Oxidation.** Cur@Fe&TA drug delivery system exhibit anti-inflammatory and antioxidant properties. To assess the modulation of the inflammatory response and oxidative stress

in the IBD mouse model, peripheral blood was collected from the mice and an enzyme-linked immunosorbent assay was performed. A significant increase in the levels of antioxidant-related cytokines (superoxide dismutase (SOD) and glutathione (GSH)) (Figure 8a,b) and down-regulation of the levels of inflammatory response-related cytokines (interleukin (IL)-6 and IL-1 $\beta$ ) were detected in all mice treated with the drug (Figure 8c,d), proving that Cur@Fe&TA exerts an anti-inflammatory and antioxidant effect to regulate the oxidative and inflammatory response of the gastrointestinal tract.

### 3. RESULTS AND DISCUSSION

IBD is a serious public health issue. However, the poor therapeutic effects and frequent adverse reactions of traditional oral drugs limit the efficacy of IBD treatments. In this study, a nanodrug delivery system capable of long-term IBD treatment was prepared in a simple manner by constructing a metal-polyphenol nanonetwork of Fe and TA to encapsulate nano-Cur. The anti-inflammatory, antioxidant, and antiapoptotic effects of the proposed Cur@Fe&TA composite nanodrug promote IBD treatment. Moreover, the composite nanodrug overcomes issues with the poor solubility and rapid drug release of traditional drugs, and the synergistic effect of the multidrug system effectively improves treatment outcomes. The Cur@Fe&TA nanomedicine delivery system exhibits good biocompatibility and can be used to treat IBD by regulating the oxidative and inflammatory response of the gastrointestinal tract. There

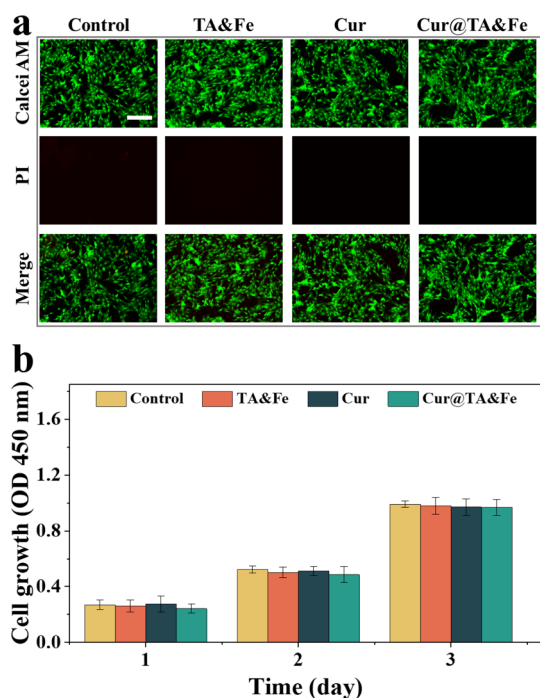


**Figure 3.** Cytotoxicity of Cur@Fe&TA. (a) Live–dead staining of BMSCs after coincubation with different drugs for 24 h. Scale bar: 200 μm. (b) CCK-8 assay results of cell growth after coincubation with different drugs for 1–3 days.

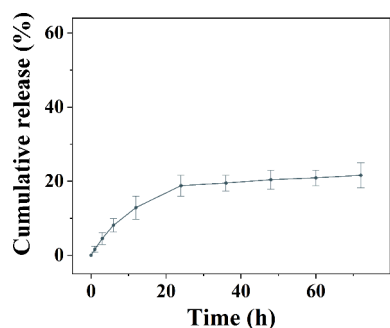


**Figure 4.** Drug release from Cur@Fe&TA in PBS.

are, of course, some shortcomings to this study. First, the cell experiments used a single cell line. Therefore, future experiments should use multiple cell lines to ensure the reliability of the results. In addition, the application of the composite nanomaterial in treating clinical diseases with a longer disease course, such as bone injury, should be explored owing to its long-lasting activity. In conclusion, the proposed Cur@Fe&TA nanomedicine delivery system exhibits excellent clinical value and research significance.

## 4. METHODS AND MATERIALS

**4.1. Materials.** Cur (≥95%), TA (≥98%), paraformaldehyde solution (4%), DSS (≥95%), FeCl<sub>3</sub> (≥99%), CHCl<sub>3</sub> (≥99%), ethyl acetate (≥95%), dimethyl sulfoxide (DMSO) (≥98.5%), and other chemicals were purchased from McLean. The purity of all chemicals meets the standard for cellular experiments. All chemicals were used as received without further purification. H&E, TUNEL, OCC, and ZO-1 staining kits were purchased from Thermo Fisher Scientific. CCK-8 and enzyme-linked immunosorbent assay (ELISA) kits were purchased from

Beyotime Biotechnology. All cells were obtained from the laboratory and were at the appropriate stage of the cell cycle for the experiment.

**4.2. Preparation of Cur@Fe&TA.** A 40 mg/mL solution of Cur in DMSO was prepared by sonication. The solution was diluted with ultrapure water under continuous sonication until Cur completely formed nanostructures. Next, a TA solution (24 mM) and FeCl<sub>3</sub> solution (40 mM) were added sequentially (Cur/TA/FeCl<sub>3</sub> = 1:2:2), and the mixture was sonicated until Cur was sufficiently captured by the metal–polyphenol network to obtain Cur@Fe&TA. The obtained mixture was dialyzed for 12 h in ultrapure water (molecular weight: 5 kDa) and then lyophilized for 24–48 h until a yellow powder was obtained. This lyophilized Cur@Fe&TA powder was used for subsequent testing.

**4.3. Particle Size and Morphology Measurements.** To evaluate the stability in aqueous solution, Cur@Fe&TA and Cur solutions were added to the same volume of CHCl<sub>3</sub> solution, and the diffusion/separation of the solutions was observed. The morphology was observed by SEM (TESCAN MIRA4 LMH) at an accelerating voltage of 20 kV and working distance of 8.88 mm. The SEM specimens were prepared by dropping the Cur@Fe&TA solution onto a silicon wafer and freeze-drying. In addition, we further observed the fine structure of nanomaterials by TEM (JEM-F200) and analyzed the elemental distribution of nanoparticles by EDS spectroscopy. The particle size and zeta potential were measured by DLS (Malvern Zetasizer Nano ZS90) at a laser wavelength of 633 nm, power of 4 mW, and temperature of 25 °C.

**4.4. Drug Loading and Encapsulation Rate Measurements.** The lyophilized powder of the nanomaterial was dissolved in 5 mL of ethyl acetate and a small amount of hydrochloric acid was added. The absorbance of curcumin in the supernatant was determined with a UV spectrophotometer (Multiskan SkyHigh, China) at 418 nm. At the same time, inductively coupled plasma–atomic emission spectrometry (Thermo element) was used to determine the content of Fe. Calculated drug loading: DLC (%) = (mass of Cur in Cur@TA&Fe complex/mass of Cur@TA&Fe complex NPs) × 100%.

First, the free curcumin was determined, the 1 mL Cur@TA&Fe sample was resuspended with ultrapure water, 5 mL of dichloromethane was added, and the extract was 5 min. The upper liquid was discarded, and the absorbance value at 418 nm was measured to calculate the concentration. Then, the total amount of curcumin was measured, and an additional 0.1 mL sample was taken to directly measure the absorbance value at 418 nm to calculate the corresponding concentration. Encapsulation efficiency (%) = [1 – (amount of free curcumin/total amount of curcumin)] × 100%.

**4.5. Cytotoxicity Measurements.** The drug powder was fully sterilized using UV light and dissolved in PBS. BMSCs with a density of  $0.5 \times 10^4$  mL<sup>-1</sup> were inoculated in 96-well plates and coincubated with 10 μL of Cur, Fe&TA, Cur@Fe&TA, or PBS (control) solution. CCK-8 assays were conducted by adding 10 μL of CCK-8 solution to each well for three consecutive days according to the CCK-8 kit operating instructions. Calcein AM/PI staining was conducted using a Calcein AM/PI staining kit after coincubation in a cell culture incubator based on the manufacturer’s instructions. At the end of the incubation period, the cells were observed under a fluorescence microscope. All experiments were repeated at least three times.

**4.6. Drug Release Measurements.** The *in vitro* drug release from Cur@Fe&TA was determined using UV absorption

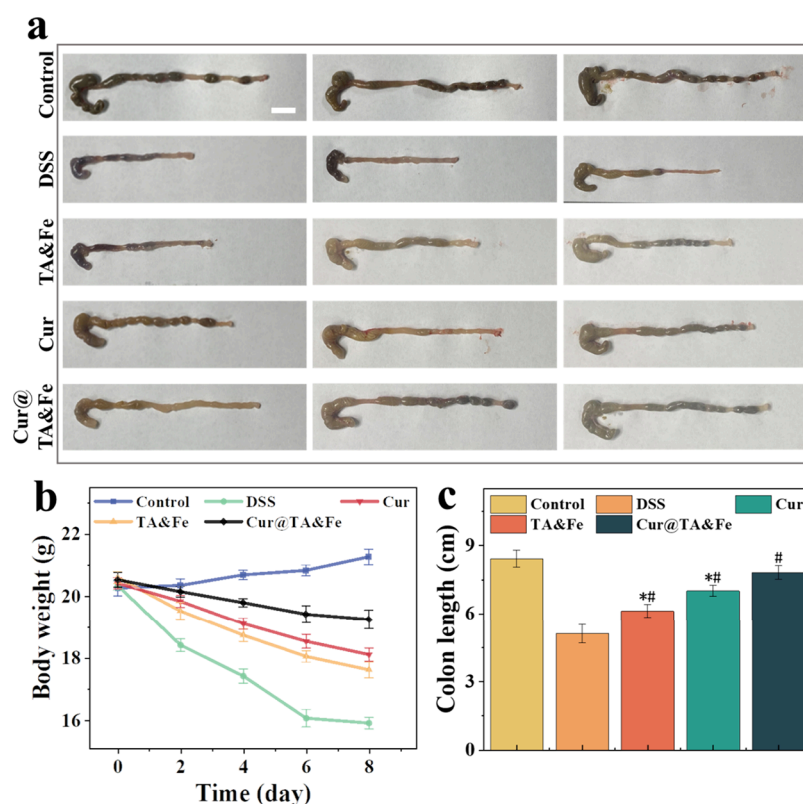


**Figure 5.** Therapeutic effect of Cur@Fe&TA in IBD mouse model. (a) Representative figures of colons, scale bar: 1 cm, (b) changes in body weight, and (c) colon lengths of mice in each experimental group.

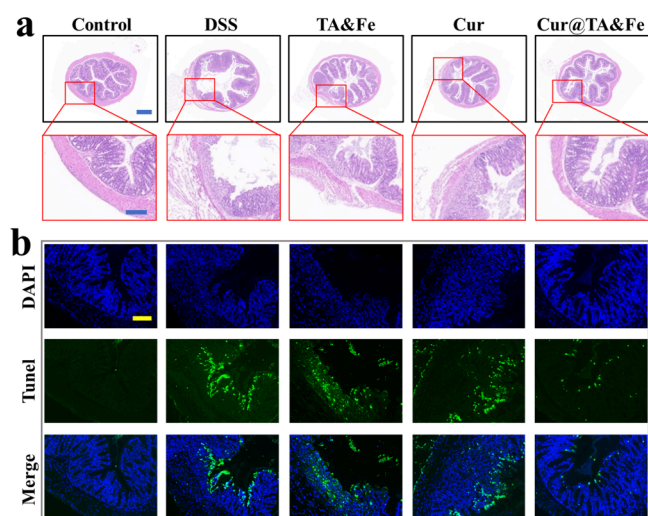


**Figure 6.** Analysis of morphological changes and apoptosis in the colon. (a) Representative H&E-stained sections of mice colons from each experimental group. Scale bars: 500  $\mu\text{m}$  (top) and 200  $\mu\text{m}$  (bottom). (b) Representative TUNEL-stained sections of mice colons from each experimental group. Scale bar: 100  $\mu\text{m}$ .

spectroscopy. We placed 1 mL of sample solution (100  $\mu\text{g}/\text{mL}$ ) in a dialysis tube (MWCO: 2 kDa) and soak in a 20 mL buffer solution containing Tween-80 (0.1% w/w) at 37  $^{\circ}\text{C}$ . At regular intervals, remove 1 mL of dialysate. Determination of concentration with UV spectrophotometer (Multiskan Sky-High, China) at 418 nm under ambient conditions. From this, the Cur release behavior of the Cur@Fe&TA nanodrug delivery system was evaluated.

**4.7. Histological, Immunohistochemical, and Fluorescent Staining Measurements.** C57BL/6 mice ( $n = 3$ ) were fed sterile water containing DSS (4 wt %) daily to prepare an IBD mouse model. Starting on the second day of modeling, 0.1 mL of the prepared nanomedicine was fed orally every other day. The body weight of the mice was measured at regular intervals. On day 8, the mice were sacrificed and colon samples were obtained and measured for length. The collected mouse colon tissues were fixed in 4% paraformaldehyde and embedded in paraffin. The samples were serially sectioned using a slicer (HM 355S Automatic Microtomes, Thermo Scientific) and stained with H&E to assess the severity of colonic injury. Tissue damage in the mice was assessed using a scoring system based on a previous study.<sup>33</sup> Additionally, the sections were incubated with fluorescent staining based on the instructions of the 4',6-diamidino-2-phenylindole (DAPI)/TUNEL, ZO-1, and OCC fluorescent staining kits followed by incubation of the corresponding fluorescent secondary antibody of the species protected from light. Next, the nuclei of the cells were restained using DAPI and analyzed by fluorescent microscopy. The fluorescence staining results of each group were quantitatively and statistically analyzed by using ImageJ.

**4.8. Biological Indicators of Inflammation Measurements.** After 8 days of drug treatment, serum samples were separated from each experimental group of mice and centrifuged at 2500 rpm and 25  $^{\circ}\text{C}$  for 10 min to remove the supernatant. The serum levels of SOD, GSH, IL-6, and IL-1 $\beta$  were detected by an ELISA (eBioscience).

**4.9. Data Analysis.** All data are expressed as the mean  $\pm$  standard deviation. Statistical differences among groups were tested using Student's  $t$  test. Statistical significance is shown as \*

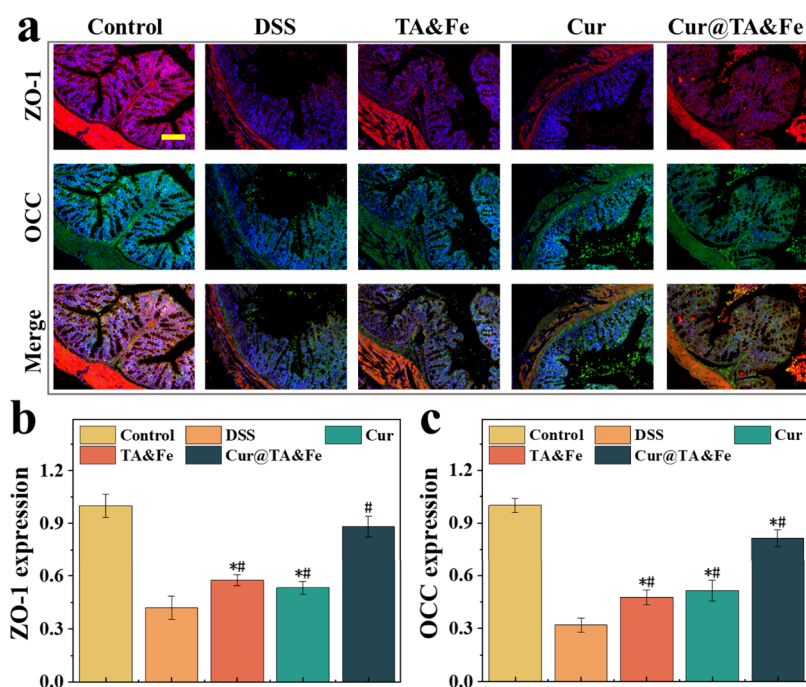


**Figure 7.** Analysis of the mucosal barrier in the IBD colon. (a) ZO-1 and OCC double-stained colonic tissues of mice in each experimental group. Scale bar: 100  $\mu\text{m}$ . Quantitative analysis of (b) ZO-1 and (c) the expression of the OCC protein expression.

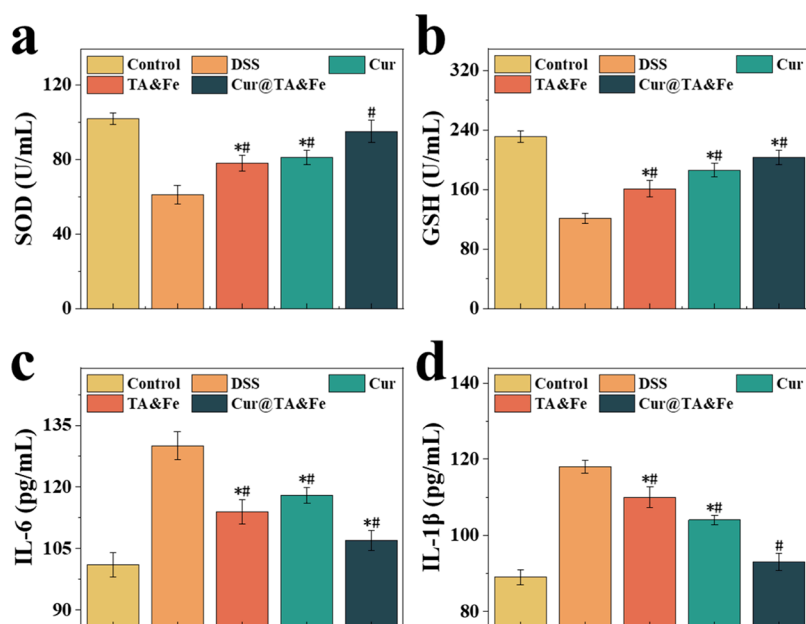


**Figure 8.** Role of Cur@Fe&TA in regulating oxidation and inflammation. (a) SOD, (b) GSH, (c) IL-6, and (d) IL-1 $\beta$  contents in the colons of mice in each experimental group.

(statistically different from the control group) or # (statistically different from the DSS group).

## Authors

**Jiman Jin** – The Third Affiliated Hospital of Wenzhou Medical University, Wenzhou 325200, China

**Xiuzhi Ye** – The Third Affiliated Hospital of Wenzhou Medical University, Wenzhou 325200, China

**Zhenfeng Huang** – The Third Affiliated Hospital of Wenzhou Medical University, Wenzhou 325200, China

Complete contact information is available at:  
<https://pubs.acs.org/10.1021/acsomega.3c10214>

## AUTHOR INFORMATION

### Corresponding Authors

**Shicui Jiang** – The Third Affiliated Hospital of Wenzhou Medical University, Wenzhou 325200, China;

Email: [shicuijiang@wmu.edu.cn](mailto:shicuijiang@wmu.edu.cn)

**Dini Lin** – The Third Affiliated Hospital of Wenzhou Medical University, Wenzhou 325200, China; [orcid.org/0009-0007-5456-7271](https://orcid.org/0009-0007-5456-7271); Email: [lindini@wmu.edu.cn](mailto:lindini@wmu.edu.cn)

## Notes

The authors declare no competing financial interest.

## ACKNOWLEDGMENTS

This work was supported by grants from Zhejiang Province Traditional Chinese Medicine Scientific Project (No.2024ZL1007).

## REFERENCES

- (1) Kaplan, G. G. The global burden of IBD: from 2015 to 2025. *Nat. Rev. Gastroenterol Hepatol* **2015**, *12* (12), 720–727. From NLM.
- (2) Singh, S.; Boland, B. S.; Jess, T.; Moore, A. A. Management of inflammatory bowel diseases in older adults. *Lancet Gastroenterol Hepatol* **2023**, *8* (4), 368–382. From NLM.
- (3) Huang, Q.; Yang, Y.; Zhu, Y.; Chen, Q.; Zhao, T.; Xiao, Z.; Wang, M.; Song, X.; Jiang, Y.; Yang, Y.; et al. Oral Metal-Free Melanin Nanozymes for Natural and Durable Targeted Treatment of Inflammatory Bowel Disease (IBD). *Small* **2023**, *19* (19), No. e2207350. From NLM.
- (4) Glassner, K. L.; Abraham, B. P.; Quigley, E. M. M. The microbiome and inflammatory bowel disease. *J. Allergy Clin Immunol* **2020**, *145* (1), 16–27. From NLM.
- (5) Gros, B.; Kaplan, G. G. Ulcerative Colitis in Adults: A Review. *Jama* **2023**, *330* (10), 951–965. From NLM.
- (6) Bisgaard, T. H.; Poulsen, G.; Allin, K. H.; Keefer, L.; Ananthakrishnan, A. N.; Jess, T. Longitudinal trajectories of anxiety, depression, and bipolar disorder in inflammatory bowel disease: a population-based cohort study. *EClinicalMedicine* **2023**, *59*, No. 101986. From NLM.
- (7) Sienkiewicz, M.; Sroka, K.; Binienda, A.; Jurk, D.; Fichna, J. A new face of old cells: An overview about the role of senescence and telomeres in inflammatory bowel diseases. *Ageing Res. Rev.* **2023**, *91*, No. 102083. From NLM.
- (8) Ona, S.; James, K.; Ananthakrishnan, A. N.; Long, M. D.; Martin, C.; Chen, W.; Mitchell, C. M. Association Between Vulvovaginal Discomfort and Activity of Inflammatory Bowel Diseases. *Clin Gastroenterol. Hepatol.* **2020**, *18* (3), 604–611. From NLM.
- (9) Sutton, T. D. S.; Clooney, A. G.; Hill, C. Giant oversights in the human gut virome. *Gut* **2020**, *69* (7), 1357–1358. From NLM.
- (10) Axelrad, J. E.; Bazarbashi, A.; Zhou, J.; Castañeda, D.; Gujral, A.; Sperling, D.; Glass, J.; Agrawal, M.; Hong, S.; Lawlor, G.; Hudesman, D.; Chang, S.; Shah, S.; Yajnik, V.; Ananthakrishnan, A.; Khalili, H.; Colombel, J. F.; Itzkowitz, S.; et al. Hormone Therapy for Cancer Is a Risk Factor for Relapse of Inflammatory Bowel Diseases. *Clin Gastroenterol. Hepatol.* **2020**, *18* (4), 872–880. From NLM.
- (11) Cunha Neto, F.; Marton, L. T.; de Marqui, S. V.; Lima, T. A.; Barbalho, S. M. Curcuminoids from *Curcuma Longa*: New adjuvants for the treatment of crohn's disease and ulcerative colitis? *Crit Rev. Food Sci. Nutr* **2019**, *59* (13), 2136–2143. From NLM.
- (12) Cheifetz, A. S.; Gianotti, R.; Lubner, R.; Gibson, P. R. Complementary and Alternative Medicines Used by Patients With Inflammatory Bowel Diseases. *Gastroenterology* **2017**, *152* (2), 415–429.e415. From NLM.
- (13) Chang, R.; Chen, L.; Qamar, M.; Wen, Y.; Li, L.; Zhang, J.; Li, X.; Assadpour, E.; Esatbeyoglu, T.; Kharazmi, M. S.; et al. The bioavailability, metabolism and microbial modulation of curcumin-loaded nanodelivery systems. *Adv. Colloid Interface Sci.* **2023**, *318*, No. 102933. From NLM.
- (14) Hu, S.; Xia, K.; Huang, X.; Zhao, Y.; Zhang, Q.; Huang, D.; Xu, W.; Chen, Z.; Wang, C.; Zhang, Z. Multifunctional CaCO<sub>3</sub>@Cur@QTX125@HA nanoparticles for effectively inhibiting growth of colorectal cancer cells. *J. Nanobiotechnology* **2023**, *21* (1), 353. From NLM.
- (15) Yang, J.; Yang, B.; Shi, J. A Nanomedicine-Enabled Ion-Exchange Strategy for Enhancing Curcumin-Based Rheumatoid Arthritis Therapy. *Angew. Chem., Int. Ed. Engl.* **2023**, *62* (44), No. e202310061. From NLM.
- (16) Joshi, P.; Bisht, A.; Paliwal, A.; Dwivedi, J.; Sharma, S. Recent updates on clinical developments of curcumin and its derivatives. *Phytother Res.* **2023**, *37* (11), 5109–5158. From NLM.
- (17) Sardou, H. S.; Vosough, P. R.; Abbaspour, M.; Akhgari, A.; Sathyapalan, T.; Sahebkar, A. A review on curcumin colon-targeted oral drug delivery systems for the treatment of inflammatory bowel disease. *Inflammopharmacology* **2023**, *31* (3), 1095–1105. From NLM.
- (18) Hao, M.; Chu, Y.; Lei, J.; Yao, Z.; Wang, P.; Chen, Z.; Wang, K.; Sang, X.; Han, X.; Wang, L.; et al. Pharmacological Mechanisms and Clinical Applications of Curcumin: Update. *Ageing Dis* **2023**, *14* (3), 716–749. From NLM.
- (19) Islam, T.; Albracht-Schulte, K.; Ramalingam, L.; Schlubritz-Lutsevich, N.; Park, O. H.; Zabet-Moghaddam, M.; Kalupahana, N. S.; Moustaid-Moussa, N. Anti-inflammatory mechanisms of polyphenols in adipose tissue: role of gut microbiota, intestinal barrier integrity and zinc homeostasis. *J. Nutr Biochem* **2023**, *115*, No. 109242. From NLM.
- (20) Guo, W.; Li, Y.; Zhu, C.; Duan, Z.; Fu, R.; Fan, D. Tannic acid-Fe(3+) dual catalysis induced rapid polymerization of injectable poly(lysine) hydrogel for infected wound healing. *Int. J. Biol. Macromol.* **2023**, *249*, No. 125911. From NLM.
- (21) Geng, H.; Zhong, Q. Z.; Li, J.; Lin, Z.; Cui, J.; Caruso, F.; Hao, J. Metal Ion-Directed Functional Metal-Phenolic Materials. *Chem. Rev.* **2022**, *122* (13), 11432–11473. From NLM.
- (22) Guo, Y.; Sun, Q.; Wu, F. G.; Dai, Y.; Chen, X. Polyphenol-Containing Nanoparticles: Synthesis, Properties, and Therapeutic Delivery. *Adv. Mater.* **2021**, *33* (22), No. e2007356. From NLM.
- (23) Shen, Y.; Yuk, S. A.; Kwon, S.; Tamam, H.; Yeo, Y.; Han, B. A timescale-guided microfluidic synthesis of tannic acid-Fe(III) network nanocapsules of hydrophobic drugs. *J. Controlled Release* **2023**, *357*, 484–497. From NLM.
- (24) Cheng, X.; Zhu, Y.; Tang, S.; Lu, R.; Zhang, X.; Li, N.; Zan, X. Material priority engineered metal-polyphenol networks: mechanism and platform for multifunctionalities. *J. Nanobiotechnology* **2022**, *20* (1), 255. From NLM.
- (25) Gong, Y.; Wang, P.; Cao, R.; Wu, J.; Ji, H.; Wang, M.; Hu, C.; Huang, P.; Wang, X. Exudate Absorbing and Antimicrobial Hydrogel Integrated with Multifunctional Curcumin-Loaded Magnesium Polyphenol Network for Facilitating Burn Wound Healing. *ACS Nano* **2023**, *17* (22), 22355–22370. From NLM.
- (26) Banerjee, S.; Chakravarty, A. R. Metal complexes of curcumin for cellular imaging, targeting, and photoinduced anticancer activity. *Acc. Chem. Res.* **2015**, *48* (7), 2075–2083. From NLM.
- (27) Chen, Z.; Farag, M. A.; Zhong, Z.; Zhang, C.; Yang, Y.; Wang, S.; Wang, Y. Multifaceted role of phyto-derived polyphenols in nanodrug delivery systems. *Adv. Drug Deliv Rev.* **2021**, *176*, No. 113870. From NLM.
- (28) Zhang, L.; McClements, D. J.; Wei, Z.; Wang, G.; Liu, X.; Liu, F. Delivery of synergistic polyphenol combinations using biopolymer-based systems: Advances in physicochemical properties, stability and bioavailability. *Crit Rev. Food Sci. Nutr* **2020**, *60* (12), 2083–2097. From NLM.
- (29) Chen, M.; Lan, H.; Jin, K.; Chen, Y. Responsive nanosystems for targeted therapy of ulcerative colitis: Current practices and future perspectives. *Drug Deliv* **2023**, *30* (1), No. 2219427. From NLM.
- (30) Naeem, M.; Awan, U. A.; Subhan, F.; Cao, J.; Hlaing, S. P.; Lee, J.; Im, E.; Jung, Y.; Yoo, J. W. Advances in colon-targeted nano-drug delivery systems: challenges and solutions. *Arch Pharm. Res.* **2020**, *43* (1), 153–169. From NLM.
- (31) Liao, Y.; Yao, Y.; Yu, Y.; Zeng, Y. Enhanced Antibacterial Activity of Curcumin by Combination With Metal Ions. *Colloid and Interface Science Communications* **2018**, *25*, 1–6.
- (32) Ho, L. W. C.; Liu, Y.; Han, R.; Bai, Q.; Choi, C. H. J. Nano-Cell Interactions of Non-Cationic Bionanomaterials. *Acc. Chem. Res.* **2019**, *52* (6), 1519–1530. From NLM.
- (33) Wirtz, S.; Popp, V.; Kindermann, M.; Gerlach, K.; Weigmann, B.; Fichtner-Feigl, S.; Neurath, M. F. Chemically induced mouse models of acute and chronic intestinal inflammation. *Nat. Protoc* **2017**, *12* (7), 1295–1309. From NLM.